Electronic Supplementary Material (ESI) for Environmental Science: Nano.

Table S1 Physicochemical properties of the ordered mesoporous carbons (o-OMCs) samples.

Samples	d_{110} (nm)	SSA ($m^2\ g^{-1}$)	S_{Micro} ($m^2\ g^{-1}$)	S_{Micro}/SSA	V_{Pore} ($cm^3\ g^{-1}$)	V_{Micro} ($cm^3\ g^{-1}$)	V_{Micro}/V_{Pore}
o-OMCs-600	8.93	701.6	253.7	0.36	0.512	0.131	0.26
o-OMCs-800	8.26	750.0	328.8	0.44	0.522	0.171	0.33
o-OMCs-1000	8.10	780.3	323.7	0.41	0.569	0.168	0.30

d_{110}: Spacing of 110 planes; SSA: Specific surface area; S_{Micro}: Micropore surface area; V_{Pore}: Pore volume; V_{Micro}: Micropore volume

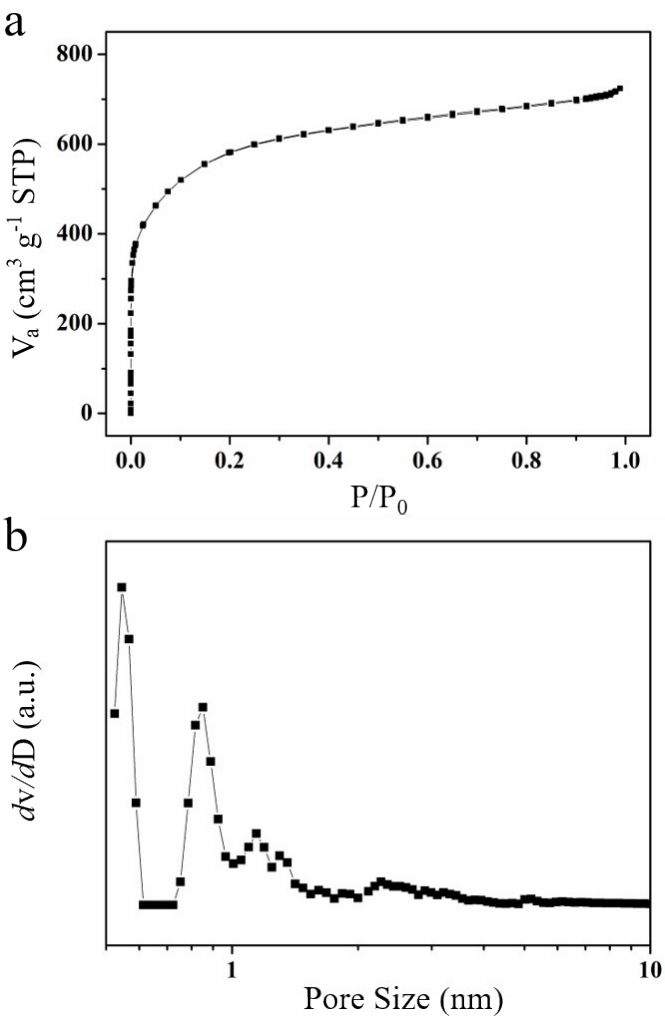

Fig. S1 (a) N_2 adsorption-desorption isotherms and (b) the corresponding pore size distribution of activated carbon (AC).

Supplementary Note for Fig. S1: Fig. S1a displays the N_2 adsorption-desorption isotherms of AC. The corresponding pore size distribution is shown in **Fig. S1b**, indicating the microporous nature of AC. The specific surface area (SSA), pore volume (V_{Pore}), and pore size of AC were analyzed and tabulated in **Table S2**. The SSA is calculated to be 1874.8 $m^2 g^{-1}$. Corresponding S_{Micro}/S_{BET} is 0.78, much higher than those of o-OMCs samples. The abundant micropores and severe pore tortuosity in AC are unfavorable for ion diffusion and usually lead to poor utilization of the inner mesopores, which consequently lead to poor desalination performance.

Table S2 Pore properties of AC.

Sample	SSA ($m^2 g^{-1}$)	S_{Micro} ($m^2 g^{-1}$)	S_{Micro}/SSA	V_{Pore} ($cm^3 g^{-1}$)	V_{Micro} ($cm^3 g^{-1}$)	V_{Micro}/V_{Pore}
AC	1874.8	1461.6	0.78	1.017	0.627	0.62

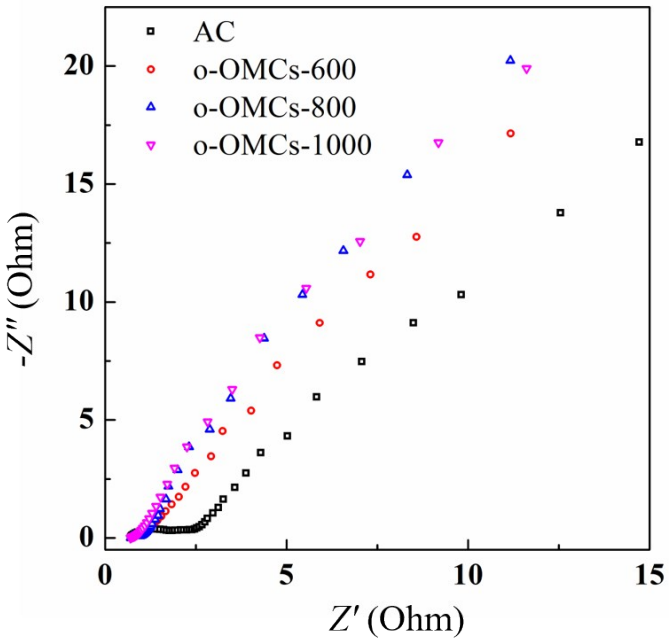

Fig. S2 Nyquist impedance spectra for AC, o-OMCs-600, o-OMCs-800 and o-OMCs-1000.

Supplementary Note for Fig. S2: Fig. S2 shows the Nyquist impedance spectra of AC, o-OMCs-600, o-OMCs-800 and o-OMCs-1000. The charge transfer resistance (R_{ct}) values are tabulated in **Table S3**. Obviously, all o-OMCs samples exhibit lower R_{ct} values than AC, indicating their improved charge transfer properties. Furthermore, o-OMCs samples also show steeper linear gradients in the upper region of the Nyquist plots (which is known as the Warburg region), providing evidence for faster ion diffusion character in the o-OMCs electrodes.

Table S3. R_{ct} values for AC, o-OMCs-600, o-OMCs-800 and o-OMCs-1000.

Sample	AC	o-OMCs-600	o-OMCs-800	o-OMCs-1000
R_{ct} (Ω)	1.83	0.72	0.67	0.58

Table S4 Comparison of o-OMCs with other mesoporous carbon-based CDI electrodes.

Type	SSA ($m^2 g^{-1}$)	Voltage (V)	Desalination capacity (mg g^{-1})	Ref.
OMC-S	1491	1.2	0.93	1
ACk2	1968	1.6	11.7	2
OMC	844	1.2	0.68	3
OMC/CNT	620.9	1.2	0.63	4
GE/MC	685.2	2.0	0.73	5
Activated MC sheets	1700	1.2	3.5	6
o-OMCs-800	750	1.0	14.58	This work

Reference

1. L. Li, L. Zou, H. Song and G. Morris, Ordered mesoporous carbons synthesized by a modified sol–gel process for electrosorptive removal of sodium chloride, *Carbon*, 2009, **47**, 775-781.
2. G. Wang, B. Qian, Q. Dong, J. Yang, Z. Zhao and J. Qiu, Highly mesoporous activated carbon electrode for capacitive deionization, *Sep. Purif. Technol.*, 2013, **103**, 216-221.
3. L. Zou, L. Li, H. Song and G. Morris, Using mesoporous carbon electrodes for brackish water desalination, *Water Res.*, 2008, **42**, 2340-2348.
4. Z. Peng, D. Zhang, L. Shi and T. Yan, High performance ordered mesoporous carbon/carbon nanotube composite electrodes for capacitive deionization, *J. Mater. Chem.*, 2012, **22**, 6603-6612.
5. D. Zhang, X. Wen, L. Shi, T. Yan and J. Zhang, Enhanced capacitive deionization of graphene/mesoporous carbon composites, *Nanoscale*, 2012, **4**, 5440-5446.
6. C. Tsouris, R. Mayes, J. Kiggans, K. Sharma, S. Yiacoumi, D. DePaoli and S. Dai, Mesoporous Carbon for Capacitive Deionization of Saline Water, *Environ. Sci. Technol.*, 2011, **45**, 10243-10249.